Postprint of: A. Krupa, B. Multan, M. Groth, K. Nyka and L. Kulas, "Autonomous Robot for Efficient Indoor RF Measurements," 2024 25th International Microwave and Radar Conference (MIKON), Wroclaw, Poland, 2024, pp. 116-121, doi: 10.23919/MIKON60251.2024.10633929.

Autonomous Robot for Efficient Indoor RF Measurements

Aleksander Krupa[1], Bartosz Multan[2], Mateusz Groth[3], Krzysztof Nyka[4], Lukasz Kulas[5]
Department of Microwave and Antenna Engineering,
Faculty of Electronics, Telecommunications and Informatics, Gdansk University of Technology 80-233 Gdansk, Poland,
[1]aleksander.krupa@pg.edu.pl, [2]bartosz.multan@pg.edu.pl, [3]mateusz.groth@pg.edu.pl, [4]krzysztof.nyka@pg.edu.pl,
[5]lukasz.kulas@pg.edu.pl,

***Abstract*—In this paper, we addresses the emergence of autonomous and semi-autonomous radio frequency (RF) measurements as a vital application for robots, particularly in indoor environments where traditional methods are labor-intensive and error-prone. We propose a method utilizing Autonomous Mobile Robots (AMRs) equipped with Light Detection and Ranging (LiDAR) and RGB-D cameras to conduct precise and repetitive RF signal measurements autonomously. The system architecture, comprising both hardware and software components, enables seamless integration and operation, reducing human intervention to preparation and analysis tasks. The proposed solution demonstrates its efficacy through experimental validation, showcasing its capability to conduct autonomous measurements with high precision and efficiency, thereby enhancing the testing of wireless communication systems and algorithms.**

***Keywords*— antenna measurements, robotic measurements, direction-of-arrival (DoA), ESPAR antenna, internet-of-things (IoT), wireless sensor networks (WSN).**

I. Introduction

With the rising complexity of hardware and software used in robotic systems, the number of possible applications also increases. With the continuous increase of available components, robotic systems become more and more popular in various applications and domains, such as health [1], search and rescue [2] or agriculture [3]. The utilization of robots increases efficiency and safety of realized tasks, especially those where high accuracy and repeatability is expected.

Autonomous and semi-autonomous RF measurements is one of the emerging applications for robots and autonomous vehicles. For example, robots can be used for implementing indoor positioning systems based on fingerprinting methods, which require a radio map of the area [4]. Additionally, such radio maps need to be periodically updated due to the changes in environment [5]. When performed by a human operator, such measurements require a significant amount of work, especially for a full scale system.

Similar measurements need to be performed for verification and validation of developed solutions based on RF devices. Not only position or direction estimation, but all other measurements where information about spatial distribution of signal is needed require similar, monotonous and time-consuming measurements which increases the risk of human error factor, especially in large areas and when the measurement grid is dense. In [6], a small unmanned surface vehicle equipped with the Global Navigation Satellite System (GNSS) was proposed. Nevertheless, such a solution cannot be applied in indoor applications where GNSS signal is unavailable although high positioning accuracy is needed. While some indoor robot navigation systems are cloud-based [7] or utilize radio frequency (RF) signals [8], they need local infrastructure installed to be able to provide information about the robot's position. There are also solutions that rely on sensor fusion to maximize the position estimation [9], [10].

This paper proposes a method for utilizing Autonomous Mobile Robots (AMRs) to conduct precise and repetitive measurements of radio signals in indoor environments. Device can be fitted with various payload accessories, thanks to its versatile mounting system. To maximize the versatility of use of the robot, we propose a self-localization solution based on information from on-board sensors. To achieve indoor autonomy the robot uses a Light Detection and Ranging (LiDAR) and a RGB-D camera [11] to execute simultaneous localization and mapping [12]. Dedicated software provides the possibility of seamless integration between robot and on-board sensors. Operators have access to tools for planning waypoint missions with multiple stops, which can be repeated numerous times. This approach reduces the occurrence of errors in RF tests compared to scenarios involving human intervention. Such a method of measurement ensures both high precision and operation without human involvement, except for preparation and analysis tasks.

II. System Architecture

A. Hardware

Proposed AMR, presented in Fig. 1, is a four wheel drive skid steering kinematics platform. Its dimensions are 46 x 49 x 32 cm and it weighs approximately 25 kg.

Fig. 1. *Measurement robot in indoor environment*

Device is powered with a 25,6 V, 20 Ah LiFePO4 battery pack, providing sufficient battery life for approximately 12 hours of continuous indoor measurements. Fig. 2 illustrates the hardware architecture of the proposed design. Robot is driven by four independent 8-inch wheel hub brushless direct-current (BLDC) motors. Each motor is controlled using a high level BLDC driver that is communicating with an on board computer using CAN protocol.

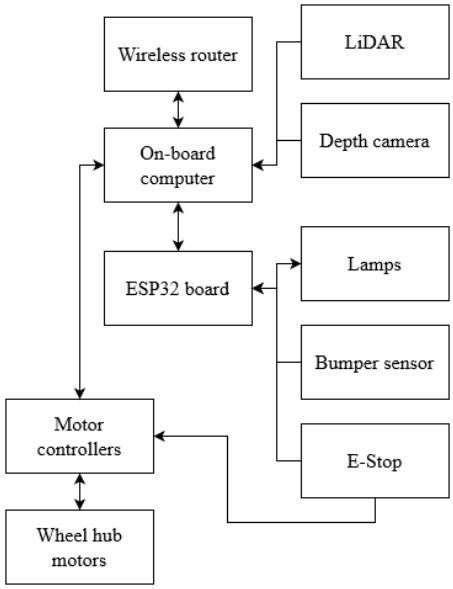

Fig. 2. Hardware architecture diagram

Robot is steered by an on-board computer with a 12th gen Intel Core i7 processor, which is necessary to provide sufficient computing power. Two main components of the robot's sensory system are 2D LiDAR located on top of the device, in the center of in-place rotation and stereoscopic depth camera located in the front part of the robot, behind the acrylic window to protect it against the elements.

Alongside the main computer, the robot is equipped with an ESP32-based microcontroller board, used for controlling low-level subsystems of the robot: lights and safety features. One of the safety features equipped within the robot is a bumper sensor: after a frontal collision, a pressure force sensor is triggering the robot to complete stop, simultaneously signaling warning with its lamps. Robot also has an emergency stop button that is connected both to motor controllers and ESP32. After pressing the button, e-stop motors instantly stop, lights are signaling error and a computer receives information about an emergency.

Robot is equipped with RGB LED lamps designed to indicate its status, aiding communication not only between robot and the operator, but also with random individuals passing by. While in motion, the robot is using a car-like scheme, with white lights at the front and red lights at the rear. During idle standing, all the lights pulsate in blue. Robot also has modes for signaling error (pulsating red), warning (pulsating orange), and conveying information to the operator regarding command execution—whether it was successful, unsuccessful, or if the command is unrecognized.

The robot facilitates seamless incorporation of various types of payload, thanks to its mounting rack system constructed from v-slot profiles with uniform spacing throughout the robot. As presented in Fig. 3, the system enables the placement of each payload plate in three locations: inside the robot, atop the robot, or at the rear external mounting frame. Additionally, the use of the common type of profiles gives the possibility for mounting non-standard components.

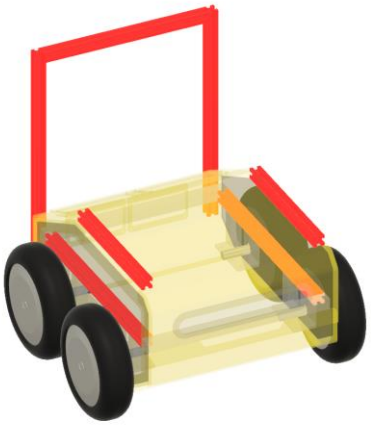

Fig. 3. Robot's payload mounting profiles

B. Software architecture

System architecture on the robot is based on Ubuntu 22.04 and Robot Operating System (ROS) Humble. Designed architecture consists of packages which can be divided in three groups: autonomous driving, measurement operation and additional features. The packages communicate with each other via publisher-subscriber model and server-client service model enabled by Robot Operating System (ROS). The architecture of the software is presented in Fig. 4.

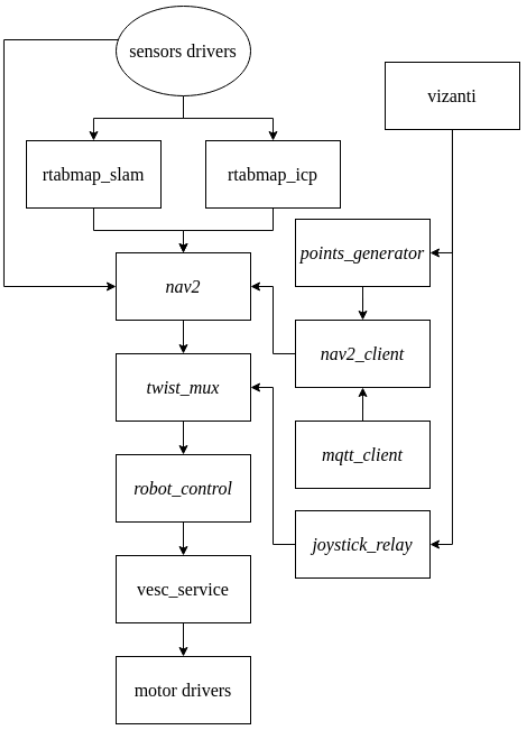

Fig. 4. Software architecture diagram

The core of the robot mobility consists of robot_control and vesc_service nodes, which allow the robot to move through velocity commands sent to the robot_control node which processes the velocity commands for left and right wheel rotation. The commands are sent to motor drivers via vesc_service node which provides CAN bus communication with the drivers. To simplify the steering, twist_mux has been used for multiplexing input from vizanti joystick and autonomy navigation commands from nav2. Vizanti is the web server enabling human operator to control the robot with a joystick.

More advanced possibilities of autonomous navigation are provided by nav2 [13] which is a navigation package for ROS, which includes many different planning and controlling algorithms. Nav2 can be used for the planning of a safe path to a given goal and execute it. It also reacts to possible difficulties occurring on the way and performs specific actions defined in a behavior tree. In this particular case, for global path planning the ThetaStar planner has been used alongside with Regulated Pure Pursuit Controller [14] for plan executing. ThetaStar creates a collision-free plan using a weight-cost function of obstacle distance and length of the path. Regulated Pure Pursuit also uses sensor data to perform collision avoidance.

To successfully plan and execute the route, nav2 needs both a map of the environment and odometry information which are provided by rtabmap_slam and rtabmap_icp packages. Those packages use LiDAR and RGB-D camera data for map and odometry creation. LiDAR is mainly used for odometry calculation with the Iterative Closest Point method providing transformation between origin map reference frame and the robot reference frame. Rtabmap_slam [11] uses lidar scans to create a 2D map with RGB-D image feature extraction for loop closing to improve map alignment and self-finding the robot on the map. Fig. 5 and Fig 6. present components of the user interface.

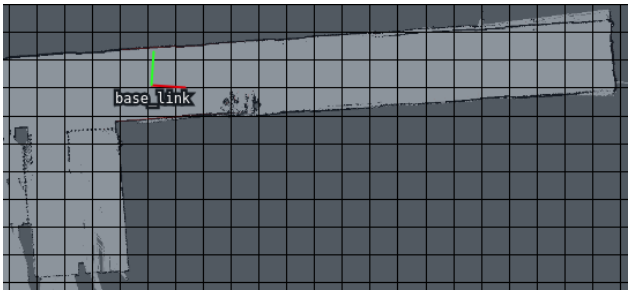

Fig. 5. Map of the corridor during the measurements

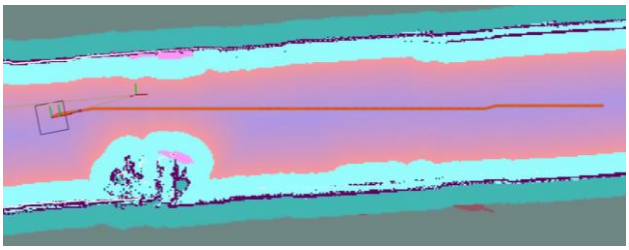

Fig. 6. Map of the corridor with obstacle cost values and generated path to given destination

The measurement abilities of the robot is provided by the nav2_client node which is responsible for mission control. Its main task is to navigate through prepared poses and react to different commands from the measurements script. Poses are given to nav2_client by points_generator node, which generates poses inside the given polygon or on the given path.

III. Operation

The robot operates in two modes - mapping and self-localization. During the mapping mode, an operator can manually navigate the robot using a joystick controller on the Vizanti interface. During the normal operation (in self-localization mode), robot operator has a several ways to set robot's destination point:

1) *Manually* - by choosing the final orientation of the robot and clicking on the desired position on a loaded map using Vizanti interface or RViZ interface.
2) *Utilizing points_generator* package, dedicated for autonomous multipoint operation. It can work in two modes:
   a) *Polygon mode*: user is selecting outline of the desired measurement region and then selecting spacing and offset from walls
   b) *Polyline mode*: user is selecting points being nodes of polyline, which represents the desired route.
3) *Adding pose to nav2_client* node for autonomous, continuous measurements via proper ROS topic

Generated positions are stored in a file, so it is possible to run tests using the same points multiple times. During the mission, the robot receives the "go to next position" command when all the measurements are finished at a specific point. When it arrives at the next point, it automatically starts the next measurement. Robot also has the capability to run

multiple test runs autonomously point by point. Fig. 7 and fig 8. illustrate self-localization error estimated in 20 consecutive measurement points.

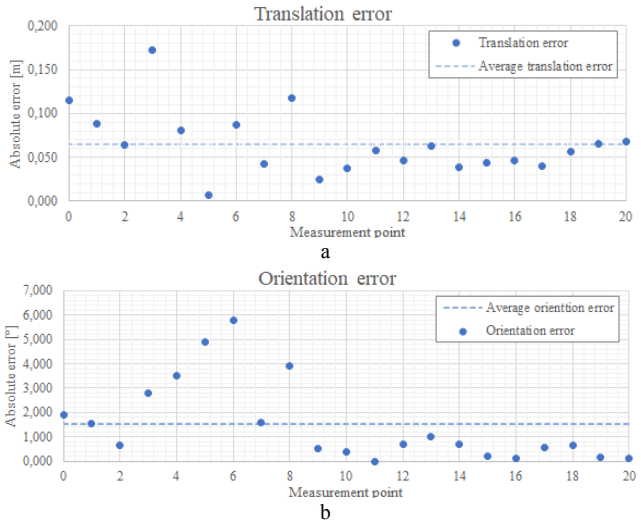

Fig. 7. Translation (a) and orientation (b) navigation error

There are two main factors limiting translation and orientation errors. One factor is the accuracy of the LiDAR sensor, which is typically ±30 mm at distances below 10 m. The other factor is the kinematic system's inability to account for precise rotational movements due to robot slippage. It leads to setting goal reaching accuracies in the controller, that ensures maximum navigation errors.

Robot is able to estimate its position with the accuracy of 5 cm using the Simultaneous Localization and Mapping (SLAM) algorithm. During the mission, goal position is considered as reached, when the robot localizes itself within a 7,5 cm radius and orientation differing maximum 17° from a given pose. In Fig. 8 an example of generated measurement poses is presented. In the figure, yellow line represents the outline of measurement mission. White circles represent nodes of the boundary. White line represents mission path and blue numerated arrows indicate measurement points.

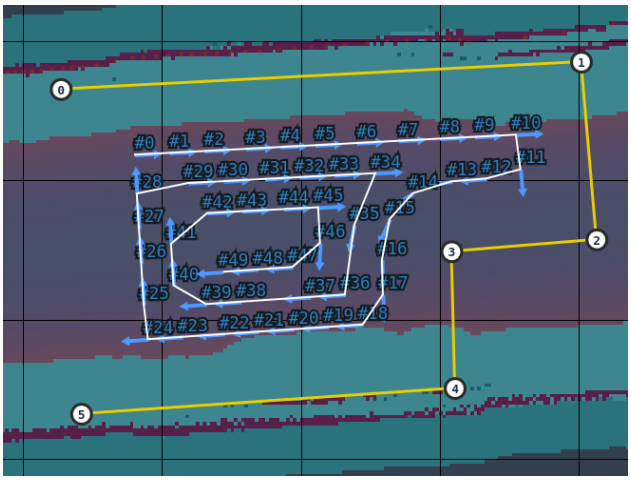

Fig. 8. Example of generated measurement poses in polygon mode

IV. Robot-Based Measurements

A. Measurement setup

To verify the robot-based measurement setup, we prepared automated and autonomous indoor Received Signal Strength (RSS) measurements of Bluetooth packets received using electronically steerable parasitic array radiator (ESPAR) [15]. The antenna was connected to a dedicated Bluetooth nRF52840-based module. For the test, the ESPAR antenna was installed 2.6 meters above the floor, on the ceiling of a 2.5 m wide corridor. The antenna was receiving Bluetooth packets using three antenna radiation patterns: omnidirectional, directional with maximum gain towards one end of the corridor, and directional with maximum gain towards the other end of the corridor. The diagram of the measurement setup is presented in Fig. 9.

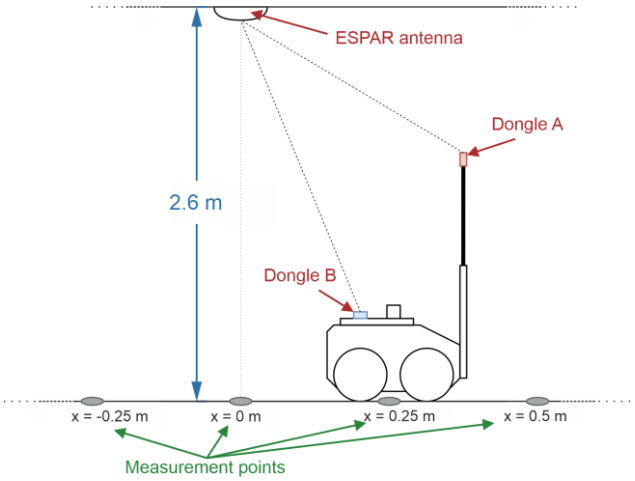

Fig. 9. Measurement scheme

Each data packet was transmitted with transmission power of 8 dBm by two NRF52840-based dedicated modules, acting as receivers, installed on the robot. First dongle, equipped with a monopole antenna, was installed on a PVC rod mounted to the rear external mounting frame at 90 cm above the ground. Second beacon with a patch antenna with maximum gain oriented towards the ceiling was mounted on the top PVC plate. During the mission, in each measurement point, 10 packets from each module and for each of three above-mentioned ESPAR radiation patterns were received before the robot continued the mission.

During the measurements, the robot performed the mission of following the waypoints, as presented in Fig. 10. Measurement points were generated on a straight line in the middle of the 2.5 m wide corridor and equally spaced 25 cm apart from each other.

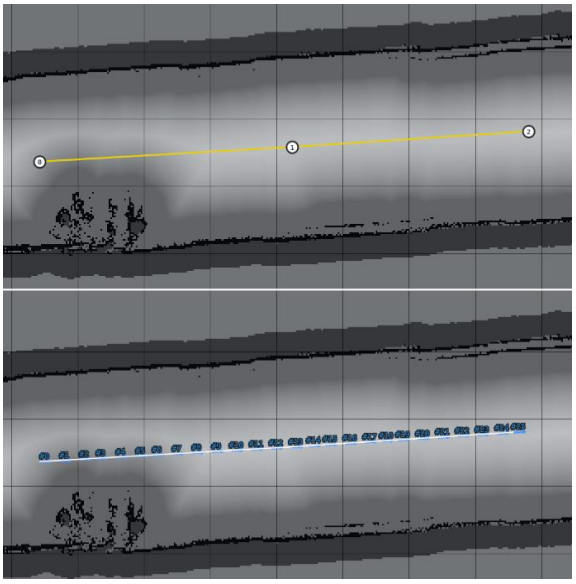

Fig. 10. Measurement points created in polyline mode alongside the corridor

Robot was moving from one measurement point to another after receiving the command that the measurements in the current position were finished. During the mission, the robot was sending its current position to the measurement script to ensure reliable validation of measurements.

B. *Results*

Measured and collected values were used for analysis of the influence of distance and chosen antenna radiation pattern on the RSS.

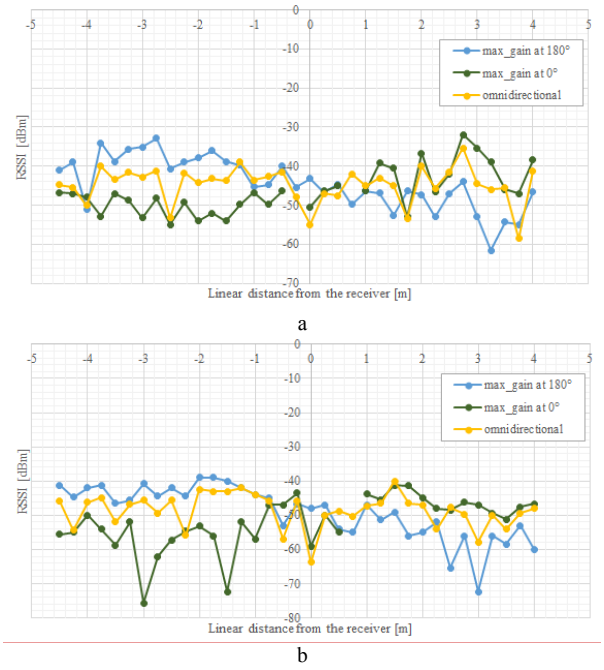

Fig. 11. RSS measurements results for monopole antenna (a) and patch antenna (b)

The results, presented in Fig. 11, show the change of RSS values in relation to the position and antenna radiation pattern. One can easily notice the difference between the received signal strength when the maximum gain of antenna characteristics was facing towards and away from the signal source. Additionally, due to the different types of antenna and different installation heights on the robot, Dongle A receives packets with approximately 10% stronger signal than Dongle B.

V. Conclusions

This paper contributes to the advancement of autonomous robotic systems for RF measurements, offering insights into hardware design, software architecture, operational modes, and experimental validation. The proposed solution addresses the challenges associated with labor-intensive and error-prone manual measurements, replacing them with enhanced and efficient automation.

By equipping AMR with LiDAR and RGB-D cameras, the proposed system can conduct precise and repetitive measurements in indoor environments without human intervention. The robot is capable of self-localization within 5 cm accuracy, reducing human errors in the measurement process.

The platform's versatility in payload integration and mounting configurations allows for seamless adaptation to various measurement tasks. Using standardized mounting profiles facilitates the integration of diverse components, thus simplifying customization and expansion.

Results validate that the system is capable of performing autonomous measurements in different environments, including smart factories and green houses, increasing the overall efficiency of testing of wireless communication systems and algorithms that can be used for direction of arrival estimation, indoor localization as well as interference mitigation.

Acknowledgment

This work has been supported by project AIMS5.0, funded from the Chips Joint Undertaking under grant agreement No 101112089 and project AGRARSENSE, funded from the Chips Joint Undertaking under grant agreement No 101095835. The JU receives support from the European Union's Horizon 2020 research and innovation programme and National Funding Authorities.

References

[1] D.-V. Bratu, M.-A. Zolya, and S.-A. Moraru, “RoboCoV Cleaner: An Indoor Autonomous UV-C Disinfection Robot with Advanced Dual-Safety Systems,” *Sensors*, vol. 24, no. 3, p. 974, Feb. 2024, doi: 10.3390/s24030974.

[2] C. Cruz Ulloa, D. Orbea, J. Del Cerro, and A. Barrientos, “Thermal, Multispectral, and RGB Vision Systems Analysis for Victim Detection in SAR Robotics,” *Applied Sciences*, vol. 14, no. 2, p. 766, Jan. 2024, doi: 10.3390/app14020766.

[3] D. A. V. Trinh and N. T. Thinh, “A Study of an Agricultural Indoor Robot for Harvesting Edible Bird Nests in Vietnam,” *AgriEngineering*, vol. 6, no. 1, pp. 113–134, Jan. 2024, doi: 10.3390/agriengineering6010008.

[4] K. Kaemarungsi and P. Krishnamurthy, “Properties of indoor received signal strength for WLAN location fingerprinting,” in *The First Annual International Conference on Mobile and Ubiquitous Systems: Networking and Services, 2004. MOBIQUITOUS 2004.*, Boston, MA, USA: IEEE, 2004, pp. 14–23. doi: 10.1109/MOBIQ.2004.1331706.

[5] L. Arvai and S. Homolya, “Efficient Radio Map Update Algorithm for Indoor Localization,” in *2020 21th International Carpathian*

Control Conference (ICCC), High Tatras, Slovakia: IEEE, Oct. 2020, pp. 1–5. doi: 10.1109/ICCC49264.2020.9257226.

[6] M. Groth, L. Kulas, K. Nyka, and Domański, Kamil, "Highly Precised and Efficient Robot-Based ESPAR Antenna Measurements in Realistic Environments [accepted]," presented at the 18th European Conference on Antennas and Propagation, Glasgow: IEEE.

[7] T. T. Khanh, T. Hoang Hai, V. Nguyen, T. D. T. Nguyen, N. Thien Thu, and E.-N. Huh, "The Practice of Cloud-based Navigation System for Indoor Robot," in *2020 14th International Conference on Ubiquitous Information Management and Communication (IMCOM)*, Taichung, Taiwan: IEEE, Jan. 2020, pp. 1–4. doi: 10.1109/IMCOM48794.2020.9001709.

[8] F. Thomas and L. Ros, "Revisiting trilateration for robot localization," *IEEE Trans. Robot.*, vol. 21, no. 1, pp. 93–101, Feb. 2005, doi: 10.1109/TRO.2004.833793.

[9] X. Tan, S. Zhang, and Q. Wu, "Research on Omnidirectional Indoor Mobile Robot System Based on Multi-sensor Fusion," in *2021 5th International Conference on Vision, Image and Signal Processing (ICVISP)*, Kuala Lumpur, Malaysia: IEEE, Dec. 2021, pp. 111–117. doi: 10.1109/ICVISP54630.2021.00028.

[10] S. Zhang, X. Tan, and Q. Wu, "Self-Positioning for Mobile Robot Indoor Navigation Based on Wheel Odometry, Inertia Measurement Unit and Ultra Wideband," in *2021 5th International Conference on Vision, Image and Signal Processing (ICVISP)*, Kuala Lumpur, Malaysia: IEEE, Dec. 2021, pp. 105–110. doi: 10.1109/ICVISP54630.2021.00027.

[11] M. Labbé and F. Michaud, "RTAB-Map as an open-source lidar and visual simultaneous localization and mapping library for large-scale and long-term online operation," *Journal of Field Robotics*, vol. 36, no. 2, pp. 416–446, Mar. 2019, doi: 10.1002/rob.21831.

[12] K. J. De Jesus, H. J. Kobs, A. R. Cukla, M. A. De Souza Leite Cuadros, and D. F. T. Gamarra, "Comparison of Visual SLAM Algorithms ORB-SLAM2, RTAB-Map and SPTAM in Internal and External Environments with ROS," in *2021 Latin American Robotics Symposium (LARS), 2021 Brazilian Symposium on Robotics (SBR), and 2021 Workshop on Robotics in Education (WRE)*, Natal, Brazil: IEEE, Oct. 2021, pp. 216–221. doi: 10.1109/LARS/SBR/WRE54079.2021.9605432.

[13] S. Macenski, F. Martin, R. White, and J. G. Clavero, "The Marathon 2: A Navigation System," in *2020 IEEE/RSJ International Conference on Intelligent Robots and Systems (IROS)*, Las Vegas, NV, USA: IEEE, Oct. 2020, pp. 2718–2725. doi: 10.1109/IROS45743.2020.9341207.

[14] S. Macenski, S. Singh, F. Martín, and J. Ginés, "Regulated pure pursuit for robot path tracking," *Auton Robot*, vol. 47, no. 6, pp. 685–694, Aug. 2023, doi: 10.1007/s10514-023-10097-6.

[15] M. Groth, M. Rzymowski, K. Nyka, and L. Kulas, "ESPAR Antenna-Based WSN Node With DoA Estimation Capability," *IEEE Access*, vol. 8, pp. 91435–91447, 2020, doi: 10.1109/ACCESS.2020.2994364.